

## THROMBOSIS AND HEMOSTASIS

# Plasmin-cleaved von Willebrand factor as a biomarker for microvascular thrombosis

Hinde El Otmani,<sup>1</sup> Rowan Frunt,<sup>1</sup> Simone Smits,<sup>1</sup> Arjan D. Barendrecht,<sup>1</sup> Steven de Maat,<sup>1,2</sup> Rob Fijnheer,<sup>3</sup> Peter J. Lenting,<sup>4</sup> and Claudia Tersteeg<sup>5</sup>

<sup>1</sup>Central Diagnostic Laboratory Research, University Medical Center Utrecht, Utrecht University, Utrecht, The Netherlands; <sup>2</sup>TargED Biopharmaceuticals, Utrecht, The Netherlands; <sup>3</sup>Department of Internal Medicine, Meander Medical Center, Amersfoort, The Netherlands; <sup>4</sup>Laboratory for Haemostasis, Inflammation and Thrombosis, INSERM Unité Mixte de Recherche 1176, Université Paris-Saclay, Le Kremlin-Bicêtre, France; and <sup>5</sup>Laboratory for Thrombosis Research, KU Leuven Campus Kulak Kortrijk, Kortrijk, Belgium

## KEY POINTS

- We developed a method to detect plasmin-cleaved VWF (cVWF) in plasma.
- cVWF forms during attacks of microthrombosis in a mouse model of thrombotic thrombocytopenic purpura and in human patients.

von Willebrand factor (VWF) is an essential contributor to microvascular thrombosis. Physiological cleavage by ADAMTS13 (a disintegrin and metalloproteinase with a thrombospondin type 1 motif, member 13) limits its prothrombotic properties, explaining why ADAMTS13 deficiency leads to attacks of microthrombosis in patients with thrombotic thrombocytopenic purpura (TTP). We previously reported that plasminogen activation takes place during TTP attacks in these patients. Furthermore, stimulation of plasminogen activation attenuates pathogenesis in preclinical TTP models *in vivo*. This suggests that plasmin is an endogenous regulator of VWF thrombogenicity, in particular when ADAMTS13 falls short to prevent microvascular occlusions. VWF cleavage by plasmin is biochemically distinct from cleavage by ADAMTS13. We hypothesized that plasmin-cleaved VWF (cVWF) holds value as a biomarker of microvascular thrombosis. Here, we describe the development of a variable domain of heavy-chain-only antibody (V<sub>H</sub>H)-based bioassay that can distinguish cVWF from intact and ADAMTS13-cleaved VWF

in plasma. We validate this assay by tracking cVWF release during degradation of microthrombi *in vitro*. We demonstrate that endogenous cVWF formation takes place in patients with TTP during acute attacks of thrombotic microangiopathy but not in those in remission. Finally, we show that therapeutic plasminogen activation in a mouse model of TTP amplifies cVWF formation, which is accompanied by VWF clearance. Our combined findings indicate that cVWF is released from microthrombi in the context of microvascular occlusion.

## Introduction

The fibrin degradation product D-dimer is widely used as a measure for ongoing fibrinolysis.<sup>1</sup> This plasmin-generated cleavage product is released during physiological hemostasis as well as during inflammation. It is therefore conventionally used as an exclusion criterion for large vessel venous thromboembolism, including pulmonary embolism and deep venous thrombosis.<sup>2</sup> However, certain forms of microvascular thrombosis are fibrin poor, making D-dimer an unattractive candidate biomarker.<sup>3</sup> Consequently, microvascular thrombosis remains devoid of an effective diagnostic and monitoring approach.

Patients suffering from thrombotic microangiopathy (TMA) experience unpredictable attacks of disseminated microvascular thrombosis. In the case of acquired thrombotic thrombocytopenic purpura (TTP) this is caused by autoimmune antibodies against the metalloprotease ADAMTS13 (a disintegrin and metalloproteinase with a thrombospondin type 1 motif, member 13).<sup>3</sup>

The constitutive cleavage of von Willebrand Factor (VWF) by ADAMTS13 is crucial for the maintenance of a normal hemostatic balance. Its deficiency in patients with TTP results in the accumulation of ultralarge VWF multimers that are prone to spontaneous platelet binding. This process drives the occurrence of life-threatening acute attacks of microvascular thrombosis that are accompanied by severe thrombocytopenia and result in end-organ damage.<sup>3</sup>

Intriguingly, complete ADAMTS13 deficiency does not lead to continuous disease in these patients and attack triggers remain elusive. However, we previously found that plasminogen activation occurs during TTP attacks, and proposed that it functions as a proteolytic rescue mechanism to clear microthrombi.<sup>4</sup> We showed in mouse models of TTP that endogenous plasmin formation mitigates the disease phenotype.<sup>5</sup> These observations prompted the development of the thrombolytic agent Microlyse for the targeted destruction of microthrombi.<sup>6</sup> Because VWF is a key component of microvascular occlusions

and because endogenous plasmin formation contributes to destruction of microthrombi in situations of endothelial distress, we, here, explored whether a soluble plasmin-generated cleavage product of VWF (cVWF) could serve as a biomarker for microvascular thrombosis. To that end, we developed a variable domain of heavy-chain-only antibody (V<sub>H</sub>H)-based bioassay. We demonstrate that this assay detects endogenous cVWF formation in patients with TTP during attack, as well as in a murine TTP disease model. Furthermore, cVWF formation coincides with VWF clearance after therapeutic plasminogen activation by Microlyse in this TTP mouse model.

## Materials and methods

An extensive description of the experimental procedures can be found in supplemental Methods, available on the *Blood* website.

### Platelet agglutination

Washed platelet suspensions were mixed with platelet aggregation inhibitors (0.55 µg/mL iloprost, 0.28 mM RGDW), and Haemate-P as a source of VWF (18 µg/mL final concentration); 220 µL of this mixture was prewarmed for 5 minutes at 37°C in an aggregometer (Chrono-log Model 700, Chrono-log Corporation, Havertown, PA) and constantly mixed by a magnetic stirrer (900 rpm). Samples' baselines were calibrated against HEPES (N-2-hydroxyethylpiperazine-N'-2-ethanesulfonic acid) Tyrode (HT) buffer and, after 1 minute, 12 µL ristocetin (at a final concentration of 800 µg/mL) was added to the platelet mix. Light transmission was measured for 30 minutes.

### Plasmin-mediated agglutinate destruction

Plasminogen was purified from human citrated plasma, as described previously.<sup>7</sup> Plasminogen (1.22 mg/mL) was activated with streptokinase (2000 IU/mL) for 15 minutes at 37°C. Six minutes after triggering of platelet agglutination with ristocetin (800 µg/mL), streptokinase-activated plasminogen (50 µL, final concentration 75 µg/mL) was added. Plasmin was inactivated at indicated time points by the addition of small-molecular protease inhibitor PPACK (5 µL, 12.5 mM working stock; 217.8 µM final concentration). Whole samples were centrifuged for 15 minutes at 400g and supernatants were collected for further analysis by western blot and enzyme-linked immunosorbent assay (ELISA).

### (c)VWF release from washed platelet agglutinates

Platelet agglutinates were formed and separated from the reaction mix (containing soluble VWF) using an 18G blunt-fill microneedle (Becton Dickinson, Franklin Lakes, NJ) attached to a 1 mL syringe (Becton Dickinson), leaving agglutinates intact. Agglutinates were washed once by the addition and subsequent aspiration of 220 µL of HT buffer containing 0.55 µg/mL iloprost, 0.28 mM RGDW, and 800 µg/mL ristocetin. After that, another 220 µL of HT buffer containing 0.55 µg/mL iloprost, 0.28 mM RGDW, and 800 µg/mL ristocetin was added and agglutinates were placed back into the aggregometer. Plasmin (50 µL, 420 µg/mL working stock; final concentration 75 µg/mL) was added and subsequently inactivated with PPACK (5 µL, 12.5 mM working stock; 217.8 µM final concentration) at indicated time points. Samples were centrifuged for 15 minutes at 400g and supernatants were collected for further analysis by western blot and ELISA.

### VWF cleavage

Lyophilized Haemate-P (plasma-derived factor VIII/VWF concentrate) was dissolved in distilled water according to the manufacturer's instructions. A 200-pg HiLoad 26/600 Superdex column (G&E Healthcare, Chicago, IL) was preequilibrated with filtration buffer (50 mM Tris; 150 mM NaCl; 5 mM Tri-sodium citrate; pH, 7.4) after which VWF-containing fractions were isolated, pooled, and buffer exchanged against phosphate-buffered saline (PBS; 21 mM Na<sub>2</sub>HPO<sub>4</sub>, 2.8 mM Na<sub>2</sub>HPO<sub>4</sub>, 140 mM NaCl; pH, 7.4) via a HiTrap desalting column (G&E Healthcare). Protein concentrations were determined via absorbance at 280 nm and confirmed by VWF antigen ELISA. Platelet-free cVWF was formed by incubating plasma-derived intact VWF (250 µg/mL) with 600 µg/mL ristocetin and 143 µg/mL streptokinase-activated-plasmin. The sample was incubated at 37°C for 1 hour. The reaction was terminated by the addition of 20 mM benzamidine and 200 mM tranexamic acid. The sample was separated by gel filtration over a HiLoad 26/600 Superdex 200-pg column (G&E Healthcare) in filtration buffer (50 mM Tris; 150 mM NaCl; 5 mM trisodium citrate; pH, 7.4). The peak corresponding to cVWF was pooled, and buffer exchanged via a HiPrep 26/10 Desalting column (G&E Healthcare) to PBS. Subsequently, the sample was flown over a lysine-sepharose column (G&E Healthcare) to remove final trace amounts of plasmin. ADAMTS13-cleaved plasma-derived VWF was kindly provided by Peter Lenting, INSERM, and characterized as previously described.<sup>8</sup>

### cVWF ELISA

*Lama glama* was immunized with plasma-derived human VWF (Haemate-P), and phage display was performed. Briefly, plasma-derived VWF was cleaved by plasmin, biotinylated, and immobilized on a microtiter plate for initial phage screening. This was followed by a second screening incorporating a depletion step with intact VWF to select the cVWF-specific capture V<sub>H</sub>H clone "G5." This capture V<sub>H</sub>H was coated onto 96-well MaxiSorp plates (5 µg/mL in PBS; 50 µL per well) overnight at 4°C. Plates were rinsed 3 times with 0.01% (volume per volume) Tween 20 in PBS (PBS-T) and then blocked with 2% (weight per volume [w/v]) bovine serum albumin (BSA) in PBS (200 µL per well) for 1 hour at room temperature (RT) while shaking, after which samples were applied. Samples were incubated at RT for 1 hour, while shaking. Nonbiotinylated cVWF was generated from VWF-containing factor VIII concentrate (Haemate-P) that was incubated with streptokinase-activated plasminogen but in the absence of ristocetin. For human and murine citrated plasma samples, assay standards were prepared in human or murine citrated normal pooled plasma (NPP), respectively, and analyzed at plasma dilutions equal to the dilutions used for the samples. Similarly, for flow experiments, in which cVWF formation by shear-unfolded VWF was studied, assay standards were prepared in endothelial growth medium.

Plates were rinsed 3 times with PBS-T, after which bound cVWF was detected with a biotinylated anti-cVWF detection V<sub>H</sub>H (clone B9; 0.05 µg/mL in 2% [w/v] BSA in PBS; 50 µL per well). Detection antibody was incubated for 1 hour at RT while shaking, after which plates were rinsed 3 times with PBS-T. An additional incubation was performed with poly-horseradish peroxidase-labeled streptavidin (diluted 4000 times in 2%

[w/v] BSA in PBS; 50  $\mu$ L per well) for 1 hour at RT while shaking, followed by 3 times washing with PBS-T. Plates were then developed by the addition of 100  $\mu$ L of 3,3',5,5'-tetramethylbenzidine substrate. Substrate development was allowed for a maximum of 30 minutes, after which 50  $\mu$ L of H<sub>2</sub>SO<sub>4</sub> (0.3 M) was added for end point absorption measurements at 450 nm. For patient plasma samples and mouse plasma samples, kinetic absorption measurements were performed every 30 seconds at 650 nm for a total duration of 30 minutes, starting immediately after the addition of 100  $\mu$ L of 3,3',5,5'-tetramethylbenzidine substrate. Results were analyzed by GraphPad Prism 9.2 using a sigmoidal 4PL fit model to which sample concentrations of cVWF were related.

### Plasma and buffer spike experiments

Citrated NPP was diluted 8 times in 2% (w/v) BSA in PBS with 200  $\mu$ M PPACK. Diluted plasma samples or buffer (2% [w/v] BSA in PBS with 200  $\mu$ M PPACK) were spiked with serially diluted intact VWF (Haemate-P) or cVWF, in the presence or absence of ristocetin (800  $\mu$ g/mL). The V<sub>H</sub>H "R2" raised against the exogenous azo-dye Reactive Red 6 was used as a negative control. Samples were analyzed for the presence of cVWF in the V<sub>H</sub>H-capture ELISA.

### Flow studies

Glass coverslips (24  $\times$  50 mm) were pretreated with glutaraldehyde.<sup>9</sup> Human umbilical vein endothelial cells (HUVECs) were cultured on coverslips in endothelial growth medium 2 supplemented with SupplementMix and gentamicin/amphotericin B mixture for a minimum of 7 days, at 37°C and 10% CO<sub>2</sub>, forming a confluent layer of cells. Coverslips were then placed in a vacuum perfusion chamber and prerinsed with endothelial growth medium 2 to prevent air from entering the chamber.<sup>10</sup> Isolated platelets ( $\pm$ 150  $\times$  10<sup>9</sup>/L) were resuspended in medium without any SupplementMix and supplemented with 1 mM histamine and 0.4  $\mu$ g/mL iloprost. Platelets were perfused over the HUVEC cells at a shear rate of 300 s<sup>-1</sup>. To enable fraction collection, this was done by pushing the platelets through the perfusion chamber, using a syringe pump holding 1 syringe containing isolated platelets, and, in parallel, a second syringe containing isolated platelets and plasmin. After 10 minutes of perfusion using the first syringe, excreted VWF strings were considered stable. The second syringe was then used to perfuse plasmin at a concentration of 50  $\mu$ g/mL over the HUVEC cells for a total duration of 13.5 minutes. Control samples were perfused with platelets in the absence of any plasmin. Simultaneously, videos were recorded at a frame rate of 1 frame per 5 seconds, and fractions of 135  $\mu$ L, corresponding with 1.5 minutes of perfusion, were collected from the flow-through in Eppendorf tubes containing 15  $\mu$ L PPACK (50  $\mu$ M final concentration). One fraction of 135  $\mu$ L was taken before the addition of plasmin to be able to determine baseline levels of (c)VWF (time = 0 minute). Samples were spun down for 15 minutes at 400g and supernatants were collected. Supernatants were diluted 4 times in 2% (w/v) BSA in PBS for analysis in cVWF and VWF antigen ELISAs.

### In vivo studies

Animal studies were performed at the Animal Research Center of KU Leuven in accordance with protocols approved by the institutional animal care and use committee (P065/2023). Eight- to 12-week-old female and male *Adamts13*<sup>-/-</sup> mice with a CASA/Rk-C57BL/6J-129X1/SvJ background were used.

Wild-type mice from this strain possess full-length ADAMTS13. *Adamts13*<sup>-/-</sup> mice with this background present with ultralarge VWF multimers. Blood was collected at baseline (7 days before TTP challenge) in trisodium citrate (5:1 volume per volume of blood: 3.2% w/v trisodium citrate). To induce TTP, mice were anesthetized using isoflurane and intravenously injected with 1000 U/kg recombinant human VWF (rhVWF; Veyvondi). All mice developed an acute TTP-like phenotype within minutes after rhVWF challenge. After 15 minutes, mice were given an intravenous injection with saline or 40  $\mu$ g Microlyse. Citrated plasma samples were obtained at 1, 2, and 4 hours after injection. Samples were diluted 4 times in block buffer for assessment in the cVWF capture ELISA. For evaluation of total VWF levels, samples were diluted 8192 times in block buffer and subjected to VWF antigen ELISA. cVWF and intact VWF, respectively, were used as reference standards. Assay standards were diluted in block buffer spiked with pooled citrated plasma from healthy control C57BL/6 mice, in the same ratio as the samples (1:4 for cVWF reference standard, and 1:8192 for VWF antigen reference standard). Results were analyzed by 2-way analysis of variance followed by the Šidák's post-hoc test.

### TTP patient studies

Citrated plasmas were obtained under informed consent from 10 healthy volunteers, 26 patients with acute TTP (collected before transfusion), and 20 patients with TTP in clinical remission (collected between 1 month and 6 years after their most recent TTP attack) with ethical approval of the University Medical Center Utrecht. Citrated plasma samples from 20 patients in remission without clinical signs of microangiopathy were collected between 1 month and 6 years after their most recent TTP attack (Table 1). Plasmin- $\alpha_2$ -antiplasmin (PAP) complexes were determined by ELISA according to the manufacturer's protocol (Technoclone, Vienna, Austria). Platelet counts were determined by hemocytometry (CELLDYN Emerald Hematology Analyzer, Abbott Laboratories, Chicago, IL). Plasma samples were diluted 8 times in block buffer for evaluation of cVWF levels by ELISA. Samples were diluted 640 times in block buffer for assessment of total VWF antigen. Assay standards were spiked with citrated NPP (1:8 for cVWF, and 1:640 for intact VWF). Results were analyzed by the Kruskal-Wallis test followed by the Dunns multiple comparisons test. Correlations were computed by Pearson correlation coefficients.

## Results

### VWF cleavage during destruction of microthrombi by plasmin

We generated microthrombi (platelet agglutinates) in vitro by incubating washed platelets with ristocetin-activated VWF. Next, we exposed these microthrombi to plasmin and performed time course sampling. We blocked plasmin activity in these samples with PPACK (supplemental Figure 1).

Microthrombus formation does not occur in the absence of VWF, and formed microthrombi do not disassemble in the absence of plasmin, indicating that these microthrombi are stable and VWF dependent (Figure 1A).

VWF migrates as a large smear with a mass >250 kDa (the size of VWF monomer) on sodium dodecyl sulfate-polyacrylamide

**Table 1. Patient and healthy donor baseline characteristics**

	N	Sex (% female)	Age (y), median (IQR)	% ADAMTS13 activity, median (IQR)	Other autoimmune disease
Acute TTP	26	77	42 (37.5-52)	0 (0-3.65)	0
Remission TTP	20	88	57 (39.5-64.5)	8.08 (3.99-30.23)	0
Normal healthy donors	10	70	34 (28-45.5)		0

IQR indicates interquartile range.

gel electrophoresis under nonreducing conditions, owing to its disulfide-linked polymeric state. Exposure to plasmin leads to a shift in this migration pattern with part of the smear being between 250 and 150 kDa (smaller than VWF monomer). Additional smaller separate fragments appear at ~120 and ~30 kDa (Figure 1B). When analyzed under reducing conditions, the 250-kDa VWF monomer is cleaved within minutes, indicating that each monomer has been cleaved at least once, without complete depolymerization (Figure 1C). Cleavage products appear at 140 and 120 kDa, and later at 110 kDa. There is progressive formation of a ~70-kDa product. This indicates that the predominant cleavage product is still polymeric and disulfide linked. A multimer analysis shows loss of larger multimers (supplemental Figure 2).

### cVWF ELISA development

Next, we set out to develop a V<sub>H</sub>H-based bioassay to track plasmin-mediated cleavage of VWF. We selected a V<sub>H</sub>H that recognizes immobilized cVWF but not intact VWF with full selectivity by phage display (capture V<sub>H</sub>H). Similarly, we identified a complementary detection of V<sub>H</sub>H that preferentially binds to cVWF.

The resulting assay setup detects cVWF, but not intact VWF, in buffer and in citrated plasma (Figure 2A-B, respectively) with a lower detection limit of ~2 ng/mL. The assay is not sensitive to the presence of ristocetin, enabling us to study cVWF release in platelet agglutination experiments. Furthermore, this assay does not recognize the presence of VWF (~10 µg/mL) or endogenous

ADAMTS13-cleaved VWF (7% of the plasma pool by estimation) in citrated plasma.<sup>8</sup> In control experiments, we confirmed the strong preference of this assay for plasmin-cleaved VWF over ADAMTS13-cleaved VWF (Figure 2C) and VWF cleavage products resulting from other proteases that are prevalent within the intravascular compartment (supplemental Figure 3).

The lack of a signal in unspiked plasma means that there is no evidence of the presence of cVWF (ie, >2 ng/mL). This is expected because plasmin-mediated VWF cleavage should only occur during (micro)vascular obstruction but not under normal physiological conditions.

### V<sub>H</sub>H binding site characterization

We made recombinant C-terminal-truncated constructs of VWF and incubated them with plasmin, as indicated (Figure 3A). Recombinant wild-type VWF forms cleavage products that are similar to those of plasma-derived VWF. When removing the C-terminal cystine-knot domain (ΔCT/CK), VWF loses its ability to form disulfide-linked multimers. Nevertheless, its cleavage products are very similar. The same holds true for further C-terminal truncation variants beyond ΔCT/CK. All these constructs can be captured by V<sub>H</sub>H G5 but only in their cleaved state (Figure 3B). However, truncation of the A2 and A3 domains (ΔA2-CT/CK) results in a strikingly different cleavage pattern and this product is no longer captured (Figure 3A-B). This indicates that domains A2 and A3 are needed for formation of the plasmin-specific cleavage product that is captured in this ELISA.

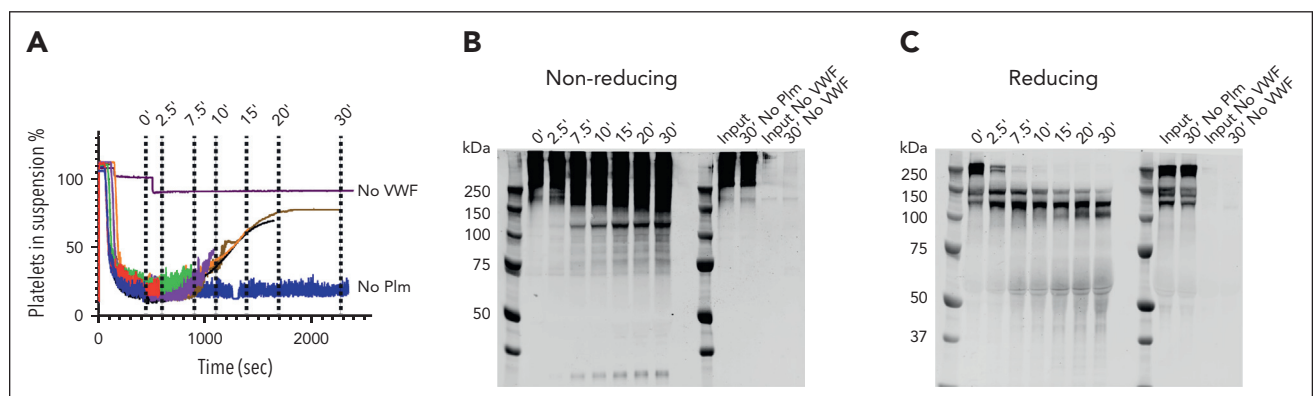


**Figure 1. Time-dependent VWF cleavage by plasmin during microthrombus breakdown.** (A) Time course of sampling during microthrombus breakdown by plasmin (75 µg/mL). Plasmin activity was blocked with PPACK, cells removed by centrifugation, and supernatants analyzed by western blotting. (B) Western blot under nonreducing conditions; (C) western blot under reducing conditions. Data represent 3 independently executed experiments. Plm, plasmin.

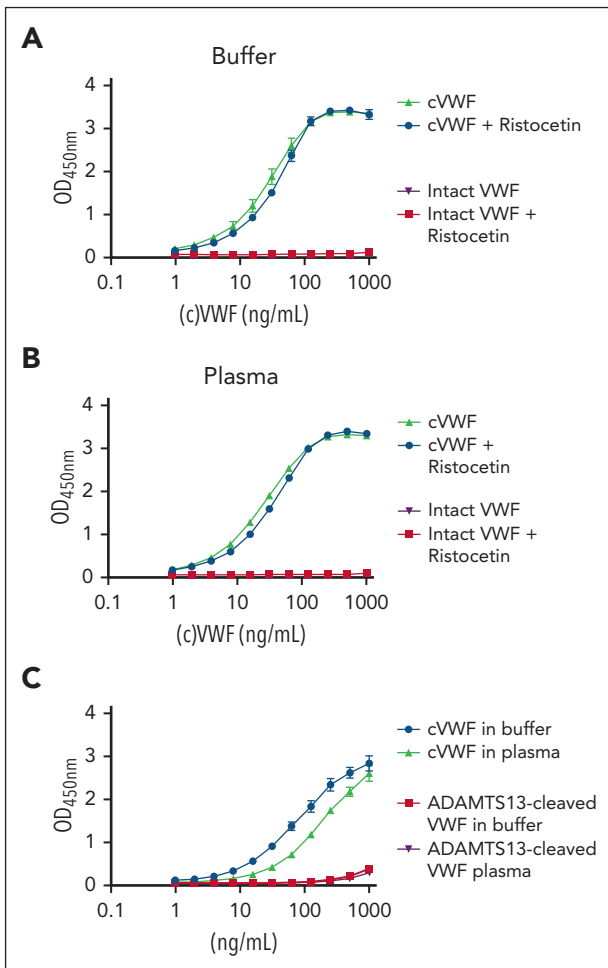


**Figure 2. cVWF assay.** (A) cVWF in buffer or (B) citrated NPP in the absence or presence of ristocetin (600  $\mu\text{g/mL}$ ). (C) cVWF or ADAMTS13-cleaved VWF in buffer or normal pooled citrated plasma. Data are expressed as means  $\pm$  standard deviation (SD) for 3 independently executed experiments.

Our first experiments indicated that plasmin cleavage of VWF results in partial depolymerization, as well as formation of soluble fragments (Figure 1). Next, we investigated which of these products were captured from spiked buffer or plasma. To that end, we eluted  $V_{\text{H}}$ -bound protein from microtiter plates with sample buffer, which we subjected to western blotting analyses. Under reducing conditions, bands at 140, 120, and 70 kDa are seen (Figure 3C). Without reduction, the smear of  $>150$  kDa is seen, as well as the 120-kDa product. The 30-kDa band present in the cVWF input material (Figure 1B) is not captured. These cleavage products are not present in unspiked plasma. These experiments indicate that a binding epitope is formed in plasmin-cleaved VWF polymers that is contained in a 120-kDa soluble fragment.

### cVWF release from microthrombi

Next, we explored whether cVWF is released during plasmin-mediated degradation of ristocetin-induced microthrombi, as displayed in Figure 1. Samples were centrifuged and platelet-free supernatants were collected for assessment of VWF antigen and cVWF levels by ELISA.

Whereas total VWF levels remain stable in the absence and presence of plasmin, ranging from  $\sim 2.5$  to  $5 \mu\text{g/mL}$  (Figure 4A),

a gradual increase in cVWF formation can be observed when plasmin is present (Figure 4B), resulting in  $\sim 40\%$  of VWF existing in a cleaved state after 30 minutes (Figure 4C).

To gain an understanding of how much cVWF is released directly from the microthrombi, we washed microthrombi to remove remaining soluble VWF and subjected them to plasmin-mediated degradation. Platelet-free supernatants were analyzed by western blotting and ELISA.

Control samples without plasmin show initial spontaneous VWF release from these complexes ( $\sim 1 \mu\text{g/mL}$ ; Figure 4D-E). In the presence of plasmin, this is  $2 \mu\text{g/mL}$  after  $\sim 10$  minutes and this additional VWF is in a cleaved state (Figure 4D-F). Approximately 50% of the VWF that is released in these experiments is cleaved (Figure 4G). These findings indicate that soluble cVWF is released from microthrombi during degradation by plasmin. We found that soluble cVWF is also released upon plasmin-mediated destruction of agonist-induced platelet aggregates (supplemental Figure 4).

### Progressive cVWF formation by shear-unfolded VWF under flow

The previous experiments were performed under static conditions, using ristocetin to unfold VWF. Next, we evaluated whether cVWF is also formed immediately after VWF secretion from endothelial cells under flow. We therefore perfused washed platelets over histamine-stimulated HUVECs to form stable platelet-covered VWF strings that were allowed to stabilize for 10 minutes, which were subsequently exposed to plasmin under flow. Samples were collected in PPACK to protect VWF from cleavage (supplemental Figure 5). The time course of 1 experiment is 13.5 minutes. One sample was taken before perfusion of plasmin or medium control to assess (c)VWF baseline levels.

Total VWF release was stable throughout experiments and comparable between plasmin-treated and control samples (30–50  $\text{ng/mL}$ ; Figure 5A). In the presence of plasmin, cVWF forms progressively, reaching a maximum concentration of  $\sim 20 \text{ ng/mL}$  (Figure 5B). Similar to the static experiments in Figure 4,  $\sim 50\%$  of VWF is cleaved in this single-pass flow model (Figure 5C).

### cVWF formation during TTP attacks in human patients

Our in vitro findings show that cVWF is released during microthrombus degradation by plasmin. We investigated whether this also occurs in patients with TTP in vivo. Our study cohort is described in Table 1, and ADAMTS13 activity levels during remission and attack are shown in supplemental Figure 6. We first observed that VWF antigen levels appear to increase in a subset of patients during TTP attacks (Figure 6A). This suggests ongoing endothelial injury or lack of VWF metabolism but fails to reach statistical significance. In contrast, cVWF levels are significantly increased in attack samples (Figure 6B), but unlike in vitro studies, on average, only 0.1% of the total plasma pool is in a plasmin-cleaved state (Figure 6C). The discriminative ability and diagnostic accuracy of cVWF are described in supplemental Figure 7 and supplemental Table 1.

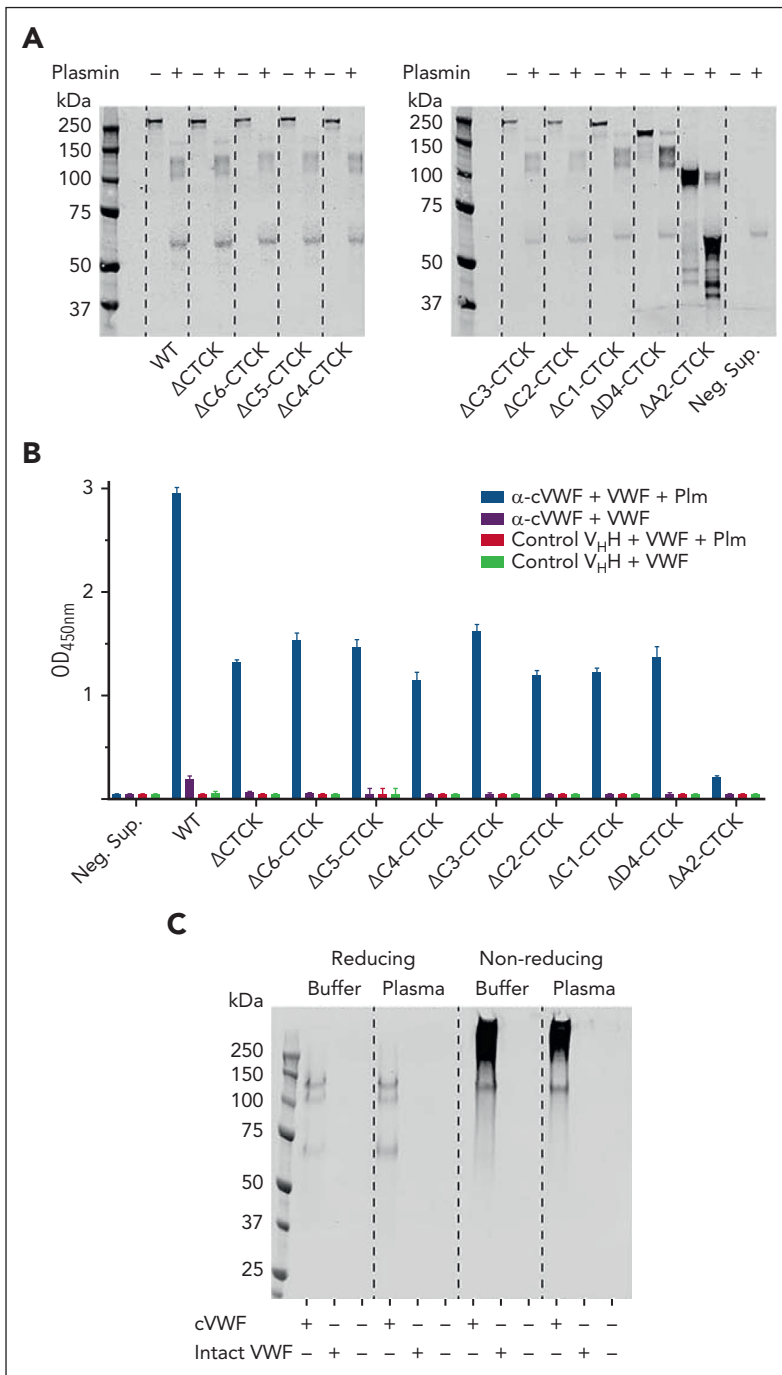


**Figure 3. Characterization of a binding site in cVWF that enables V<sub>H</sub>H capture.** Conditioned cell culture supernatants containing C-terminally truncated VWF variants were incubated with plasmin (150 μg/mL) or vehicle and analyzed by (A) western blotting and by ELISA. (B) V<sub>H</sub>H G5 was immobilized, and captured VWF variants were detected with a polyclonal antibody. (C) Western blot of captured VWF products, spiked in buffer or NPP. Data represent 3 independently executed experiments. Bar graphs show means ± SD. M, marker; Neg. Sup, negative control supernatant; Plm, plasmin.

We previously reported that PAP complex levels, a marker for plasminogen activation, are increased during TTP attacks.<sup>4</sup> In our study cohort, there is moderate negative correlation between PAP complexes and platelet counts. Patients with acute attacks generally have deep thrombocytopenia and elevated PAP complex levels in plasma (Figure 6D;  $R^2 = 0.44$ ). Accordingly, patients with thrombocytopenia with TTP have increased cVWF levels (Figure 6E;  $R^2 = 0.40$ ). The presence of increased PAP levels strongly correlates with cVWF levels (Figure 6F), indicating that plasmin is likely responsible for VWF cleavage in vivo during TTP attacks. There is no correlation between VWF antigen levels and cVWF levels, platelet counts,

or PAP complex levels (Figure 6G-I, respectively). This implies that TMA, rather than increased VWF levels, is the driving force behind endogenous cVWF production.

### Therapeutic plasminogen activation accelerates cVWF production in a TTP mouse model

Next, we explored the impact of therapeutic plasminogen activation on cVWF production in a mouse model for TTP. We challenged *Adams13*<sup>-/-</sup> mice with rhVWF. Fifteen minutes after this challenge, saline or the VWF-targeting plasminogen activator Microlyse was administered, and blood was collected at several consecutive time points.

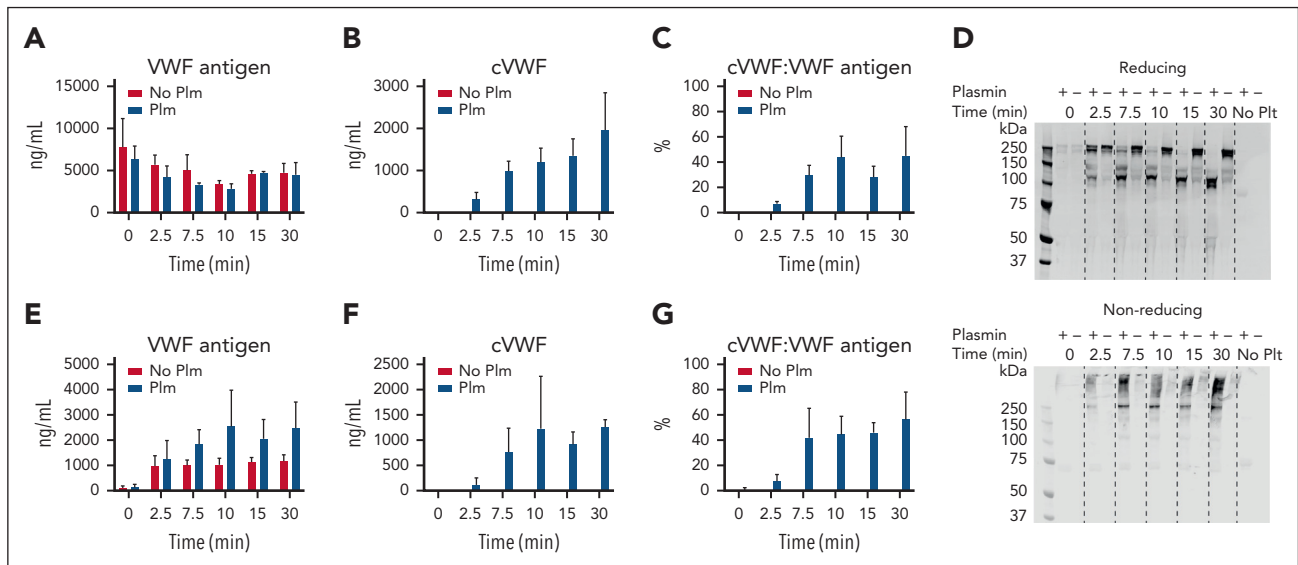


**Figure 4. cVWF release from microthrombi.** Microthrombi were exposed to plasmin (75  $\mu\text{g}/\text{mL}$ ) or buffer. (A-C) Platelet-free supernatants were collected and analyzed by ELISA. Next, preformed microthrombi were separated from soluble VWF by centrifugation and subjected to either degradation by plasmin (75  $\mu\text{g}/\text{mL}$ ) or buffer. Platelet complexes were removed by a second centrifugation step and supernatants analyzed by western blotting (D) and ELISA (E-G). Data represent 3 independently executed experiments. Bar graphs show means  $\pm$  SD. No Plt, no platelets; Plm, plasmin.

We found that Microlyse treatment leads to progressive VWF clearance compared with saline administration (Figure 7A). This is accompanied by a steep rise in cVWF formation after 1 hour (Figure 7B). Similar to human patients with TTP (Figure 6), endogenous cVWF production takes place in saline-treated mice. During these experiments, the fraction of VWF in a plasmin-cleaved state is approximately twice as high in Microlyse-treated mice than in saline controls (Figure 7C). Together, these data indicate that therapeutic plasminogen activation accelerates rhVWF clearance, which is accompanied by increased cVWF formation.

## Discussion

In this study, we describe the identification of cVWF as a biomarker for degradation of microthrombi. We generated a  $V_H\text{-H}$ -based bioassay and characterized it *in vitro*, in biochemical and cell biological experiments. With this assay, we demonstrated that cVWF formation takes place in patients with TTP during attacks of

TMA. Furthermore, we show that therapeutic plasminogen activation is accompanied by increased cVWF production.

Circulating VWF is predominantly secreted by endothelial cells. The metalloprotease ADAMTS13 regulates its thrombogenicity by cleavage of its A2 domain. We show that the assay displays a strong preference for cVWF over ADAMTS13-cleaved VWF. This confirms that the cleavage product resulting from plasmin-mediated VWF degradation is biochemically distinct from ADAMTS13-cleaved VWF.

We observed that cVWF is not detectable in normal plasma or in the plasma of patients with TTP during remission. This strengthens the notion that cVWF is only formed during conditions of severe endothelial distress, triggered by spontaneous microthrombus formation, and causing hypoxia-driven endothelial urokinase-type plasminogen activator receptor upregulation and subsequent plasmin activation.<sup>4</sup> Accordingly, cVWF levels are elevated in patients with TTP during attacks, and correlate with disease activity. In these patients,  $\sim 0.1\%$  of all circulating VWF

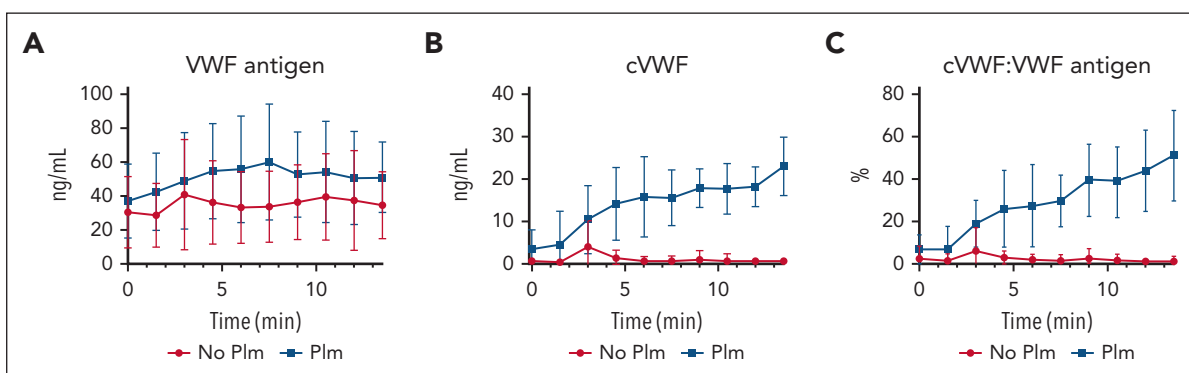


**Figure 5. cVWF formation under flow.** (A-C) Washed platelets were perfused over histamine-stimulated HUVECs. After being stable for 10 minutes, HUVEC-bound platelet-covered VWF strings were exposed to plasmin (50  $\mu\text{g}/\text{mL}$ ) or vehicle control under flow. Samples were collected into PPACK and analyzed by ELISA for VWF antigen levels, cVWF levels, and fraction of VWF in a plasmin-cleaved state. Data represent 5 independently executed experiments, and are shown as means  $\pm$  SD.

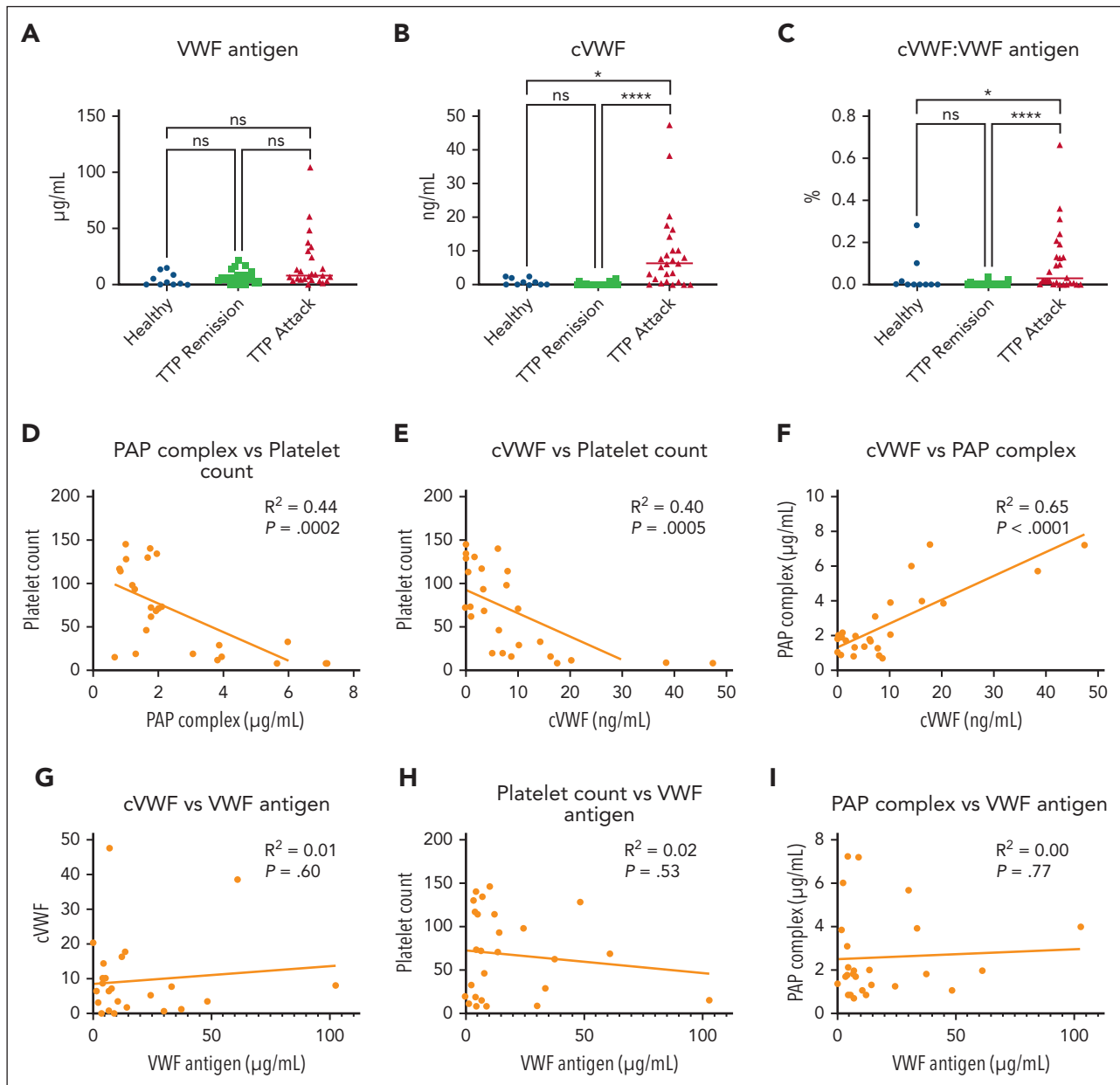


**Figure 6. cVWF formation during TMA attacks in patients with TTP.** (A-C) VWF antigen levels, cVWF levels, and fraction of VWF in a plasmin-cleaved state in healthy controls, patients with TTP in remission, and during acute attacks. Data represent 3 independently executed experiments and are shown as scatter plots with medians. Data were analyzed with the Kruskal-Wallis test followed by the Dunn multiple comparisons test. \* $P < .05$ ; \*\*\*\* $P < .0001$ ; ns, nonsignificant. (D-F) Correlations between PAP complex levels and platelet counts (D), cVWF levels and platelet counts (E), and cVWF levels and PAP complex levels (F). (G-I) Correlations between VWF antigen and cVWF levels (G), VWF antigen levels and platelet counts (H), and VWF antigen levels and PAP complex levels (I). Correlations were computed by Pearson correlation coefficients. Healthy, healthy controls.

exists in a plasmin-cleaved state. This is much lower than the cVWF levels observed in agglutination and single-pass flow studies, which reach up to 50% of the total VWF concentration. A possible explanation may be that these in vitro studies involve relatively high plasmin concentrations in the absence of clearance mechanisms and physiological inhibitors that control plasminogen activation. Plasminogen activation during endothelial distress likely occurs locally, proportionately resulting in low circulating levels of cVWF. In good correspondence, VWF antigen levels remain high in patients with acute TTP with deep thrombocytopenia, suggesting that only a small fraction of circulating VWF actively contributes to microvascular occlusions. Variations in cVWF levels during active disease may be attributable to

differences in disease severity or variabilities in the levels of plasmin(ogen) modulators. PAP complexes, plasminogen activator inhibitor-1 (PAI-1) and urokinase-type plasminogen activator (uPA) levels are known to differ among patients with TTP,<sup>4</sup> which may explain why cVWF, as a plasmin-generated cleavage product, also displays fluctuations. A long circulating half-life is an advantageous property for biomarkers.<sup>11</sup> This, for example, is the case for D-dimer, but this biomarker lacks specificity toward a pathological state. Our studies in *Adams13*<sup>-/-</sup> mice confirm that therapeutic plasminogen activation with Microlyse leads to rapid clearance of the administered rhVWF. In previous studies, we showed that endogenous VWF levels remain unaffected by Microlyse.<sup>6</sup> Only a small fraction of the remaining rhVWF



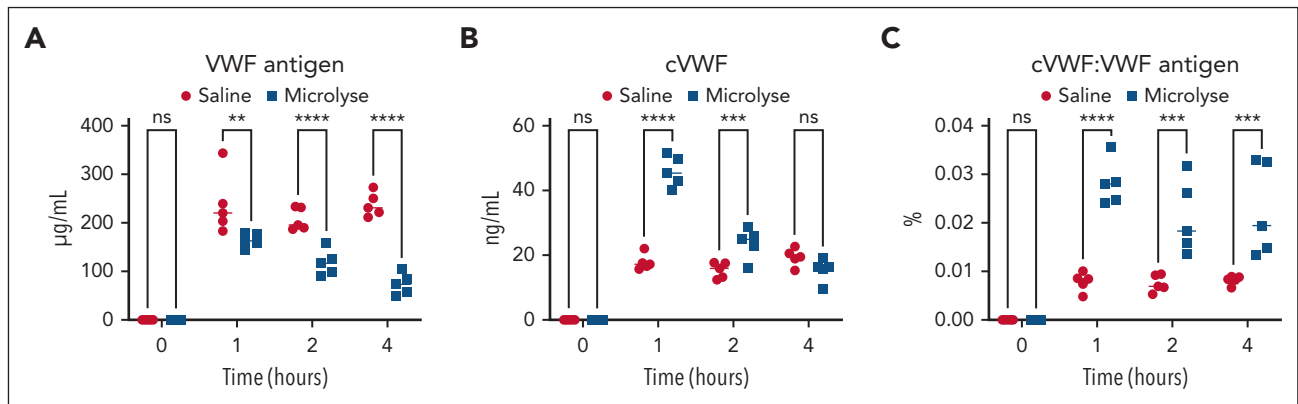


**Figure 7. Therapeutic plasminogen activation accelerates cVWF formation.** Levels of VWF antigen (A), cVWF (B), and fraction of circulating VWF that exists in a plasmin-cleaved state (C) after Microlyse treatment (blue squares) or saline treatment (red circles) in *Adams13*<sup>-/-</sup> mice, challenged by administration of rhVWF. Data are displayed as scatter plots with medians, and represent 3 independently executed experiments. Results were analyzed by 2-way analysis of variance followed by the Šidák's post-hoc test. \*\**P* < .005; \*\*\**P* < .0005; \*\*\*\**P* < .0001; ns, nonsignificant.

circulates in a cleaved state, suggesting that cVWF is relatively short lived. Our observations in patients with acute TTP show comparable endogenous cVWF levels, despite the fact that their VWF antigen levels are not raised to the extent observed in the TTP mouse model. Combined, this suggests that cVWF, in contrast to D-dimer, has positive discriminatory properties that are highly specific for an ongoing localized disease process.

VWF is regarded as a driving factor in a multitude of pathologies involving endothelial dysfunction.<sup>12</sup> It is therefore conceivable that cVWF formation also occurs in other forms of TMA or even fibrin-dependent forms of thrombosis with an imbalance between VWF and ADAMTS13. This skewed balance is known to occur in transplant-associated TMA,<sup>13</sup> in patients admitted to the intensive care unit for (non)septic disease,<sup>14</sup> and during severe acute respiratory syndrome coronavirus 2 infection.<sup>15</sup> Reduced expression of the plasminogen gene could also pose a significant risk factor for TMA development, as may occur in atypical hemolytic uremic syndrome.<sup>16</sup> This might act as an independent risk factor or contribute to disease development alongside ADAMTS13 deficiency. Insufficient VWF modulation is also a recognized contributor to more common macrovascular thrombotic events, like acute ischemic stroke and venous thromboembolism.<sup>17,18</sup>

In conclusion, we propose that cVWF is a cleavage product of VWF that reflects microvascular occlusion.

## Acknowledgments

The authors gratefully acknowledge Raymond M. Schiffelers, Rolf T. Urbanus, Marcel Fens, Arnold Koekman, and Jasper Kers.

This work was supported by a PPP Allowance from the Ministry of Economic Affairs of the Netherlands, made available by the Top Sector Life Sciences & Health to stimulate public-private partnerships.

## REFERENCES

- Righini M, Van Es J, Den Exter PL, et al. Age-adjusted D-dimer cutoff levels to rule out pulmonary embolism: the ADJUST-PE study. *J Am Med Assoc.* 2014;311(11):1117-1124.
- Favresse J, Lippi G, Roy PM, et al. D-dimer: preanalytical, analytical, postanalytical

variables, and clinical applications. *Crit Rev Clin Lab Sci.* 2018;55(8):548-577.

- Sadler JE. Pathophysiology of thrombotic thrombocytopenic purpura. *Blood.* 2017; 130(10):1181-1188.
- Tersteeg C, De Maat S, De Meyer SF, et al. Plasmin cleavage of von willebrand factor as

an emergency bypass for ADAMTS13 deficiency in thrombotic microangiopathy. *Circulation.* 2014;129(12):1320-1331.

- Tersteeg C, Joly BS, Gils A, et al. Amplified endogenous plasmin activity resolves acute thrombotic thrombocytopenic purpura in mice. *J Thromb Haemost.* 2017;15(12):2432-2442.

## Authorship

Contribution: H.E.O., R.F., S.S., A.D.B., and S.d.M. performed in vitro experiments; P.J.L. and R.F. provided essential reagents; C.T. performed the in vivo TTP model; and H.E.O., R.F., S.d.M., and C.T. wrote the manuscript.

Conflict-of-interest disclosure: S.d.M. is a cofounder of TargED Biopharmaceuticals BV, a biotech spinout company of University Medical Center Utrecht, and participates in revenue sharing as inventor through the commercialization arm of the University Medical Center Utrecht. The results discussed in this article form part of a pending patent application. The remaining authors declare no competing financial interests.

ORCID profiles: H.E.O., 0000-0002-2344-6027; R. Frunt, 0000-0001-8283-273X; S.S., 0000-0002-3229-7238; A.D.B., 0000-0002-0653-5538; S.d.M., 0000-0003-1179-374X; R. Fijnheer, 0000-0002-7844-4774; P.J.L., 0000-0002-7937-3429; C.T., 0000-0002-6380-6349.

Correspondence: Hinde El Otmani, University Medical Center Utrecht, Heidelberglaan 100, 3584 CX Utrecht, The Netherlands; email: [h.elotmani-2@umcutrecht.nl](mailto:h.elotmani-2@umcutrecht.nl).

## Footnotes

Submitted 30 May 2023; accepted 20 January 2024; prepublished online on *Blood* First Edition 25 January 2024. <https://doi.org/10.1182/blood.2023021265>.

Data are available upon reasonable request to corresponding author Hinde El Otmani ([h.elotmani-2@umcutrecht.nl](mailto:h.elotmani-2@umcutrecht.nl)).

The online version of this article contains a data supplement.

There is a [Blood Commentary](#) on this article in this issue.

The publication costs of this article were defrayed in part by page charge payment. Therefore, and solely to indicate this fact, this article is hereby marked "advertisement" in accordance with 18 USC section 1734.

6. de Maat S, Clark CC, Barendrecht AD, et al. Microlyse: a thrombolytic agent that targets VWF for clearance of microvascular thrombosis. *Blood*. 2022;139(4):597-607.
7. de Maat S, Björkqvist J, Suffritti C, et al. Plasmin is a natural trigger for bradykinin production in patients with hereditary angioedema with factor XII mutations. *J Allergy Clin Immunol*. 2016;138(5):1414-1423.e9.
8. Kizlik-Masson C, Peyron I, Gangnard S, et al. A nanobody against the von Willebrand factor A3-domain detects ADAMTS13-induced proteolysis in congenital & acquired VWD. *Blood*. 2023;141(12):1457-1468.
9. Martínez-Jothar L, Barendrecht AD, de Graaff AM, et al. Endothelial cell targeting by cRGD-functionalized polymeric nanoparticles under static and flow conditions. *Nanomaterials (Basel)*. 2020;10(7):1353.
10. Barendrecht AD, Verhoef JJF, Pignatelli S, Pasterkamp G, Heijnen HFG, Maas C. Live-cell imaging of platelet degranulation and secretion under flow. *J Vis Exp*. 2017; 2017(125):55658.
11. Kaplan AP, Maas C. The search for biomarkers in hereditary angioedema. *Front Med*. 2017;4:206.
12. Vischer UM. von Willebrand factor, endothelial dysfunction, and cardiovascular disease. *J Thromb Haemost*. 2006;4(6):1186-1193.
13. Xu Z, Luo C, Lai P, et al. von Willebrand factor as a predictor for transplant-associated thrombotic microangiopathy. *Clin Appl Thromb Hemost*. 2020;26: 1076029619892684.
14. Singh K, Kwong AC, Madarati H, et al. Characterization of ADAMTS13 and von Willebrand factor levels in septic and non-septic ICU patients. *PLoS One*. 2021;16(2): e0247017.
15. Mancini I, Baronciani L, Artoni A, et al. The ADAMTS13-von Willebrand factor axis in COVID-19 patients. *J Thromb Haemost*. 2021;19(2):513-521.
16. Bu F, Maga T, Meyer NC, et al. Comprehensive genetic analysis of complement and coagulation genes in atypical hemolytic uremic syndrome. *J Am Soc Nephrol*. 2014;25(1):55-64.
17. Wieberdink RG, Van Schie MC, Koudstaal PJ, et al. High von Willebrand factor levels increase the risk of stroke: the Rotterdam study. *Stroke*. 2010;41(10): 2151-2156.
18. Edvardsen MS, Hansen E-S, Ueland T, et al. Impact of the von Willebrand factor ADAMTS13 axis on the risk of future venous thromboembolism. *J Thromb Haemost*. 2023;21(5):1227-1237.

© 2024 American Society of Hematology. Published by Elsevier Inc. Licensed under Creative Commons Attribution-NonCommercial-NoDerivatives 4.0 International (CC BY-NC-ND 4.0), permitting only noncommercial, nonderivative use with attribution. All other rights reserved.